# A FAMILY OF IMPROVED LINAC BUNCHERS

R. Beringer and R. L. Gluckstern
Brookhaven National Laboratory and Yale University

Conventional bunchers use one or more gaps excited with fundamental frequency sinusoidal fields. They can be designed to inject about 2/3 of the dc beam into the admittance of a conventional drift-tube linac. However, the remainder of the particles (long tails) are not accelerated to the end of a long linac and will give rise to undesirable radiation and possible confusion in the beam-pickup instrumentation of a sophisticated multicavity linac.

Bunchers having several gaps with harmonically related sinusoidal fields[1, 3] are somewhat better but still have long tails. They are approximations to the saw-tooth buncher[1, 2, 3, 4] which has no tails and which can bunch all of the dc beam.

Unfortunately, no one seems to have a practical way of exciting a saw-tooth gap at frequencies as high as 200 Mc/s. Thus, other solutions are of interest.

The bunchers described here use an rf deflector to separate phase regions in space so that each phase region can be bunched independently with a sinusoidal field.

## 1. Isochronous Deflector

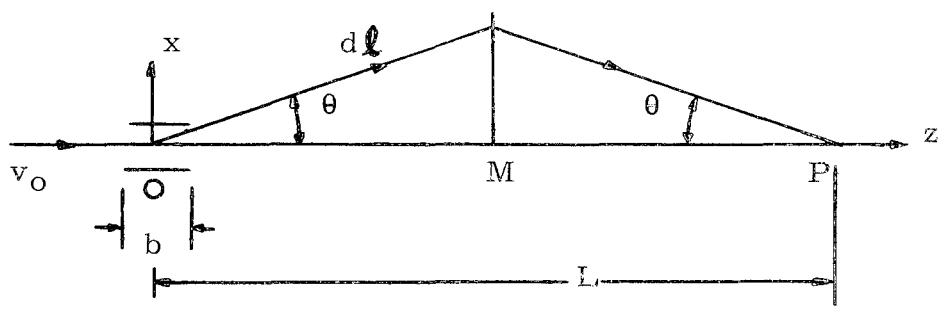

Consider an rf deflector at 0 with $E_x = E_o \sin \omega t$. The deflection angle is

$$\tan \theta = \frac{v_x}{v_o} = \frac{eE_o b}{mv_o^2} \sin \omega t ,$$

where dimension b includes a transit-time factor. M is a magnetic or electrostatic lens of unit magnification. If we approximate it as a thin lens, the elapsed time from 0 to P is

$$\frac{1}{v} \int_o^P d\ell = \frac{1}{\sqrt{v_o^2 + v_x^2}} \frac{L}{\cos \theta} = \frac{L}{v_o} .$$

Thus the system is isochronous.

2. Isochronous Deflector - Redeflector

The angles $\theta$ at P can be eliminated by a second deflector since the system is isochronous. The particle arrives at P at time $t + L/v_o$ with transverse velocity $v_x = -(eE_o b/mv_o) \sin \omega t$. If we excite an identical deflector with field $E_x = E_o \sin (\omega t - \omega L/v_o)$, then all axial

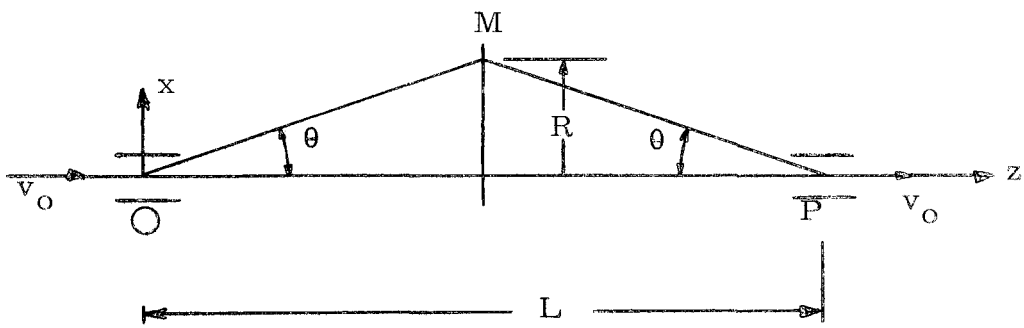


particles leave P with velocity $v_o$ along z. This isochronous transport is also true for nonaxial particles incident at 0. Further, the field $E_x$ need not be uniform over the aperture but only the same in the two deflectors provided that they are symmetrically placed with respect to M.

Phase errors $\Delta(\omega L/v_o) = -(\omega L/v_o)(\Delta v_o/v_o)$ arising from variations in $v_o$ (dc preinjector voltage changes) give angular errors in the redeflected beam. These should be small compared to beam-emittance angles. The maximum angular error is

$$\frac{\Delta\theta_{max}}{\theta} = \frac{(\Delta v_x)_{max}}{v_o} = \frac{2\omega R}{v_o}\,\frac{\Delta v_o}{v_o} \quad .$$

It is independent of L for a given maximum deflection R. In a typical case the errors are about one milliradian.

3. Deflector - Redeflector and a Bunching Gap

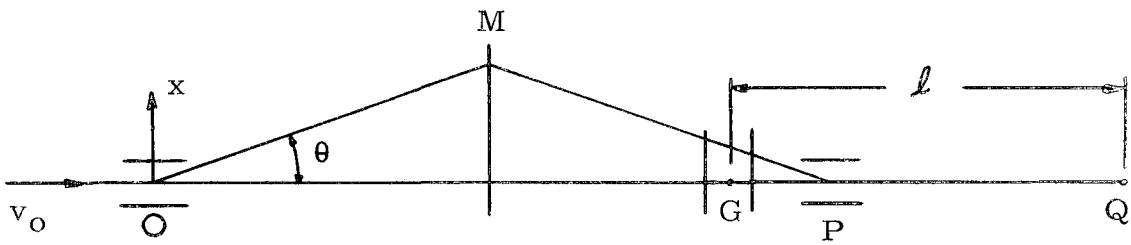


Near P, where the beam is still separated in space, we place a bunching gap with rf voltage

$$gE_z = -V_o \cos \omega t \, .$$

Particles leaving the gap have velocity

$$v = \sqrt{v_o^2 (1 + \tan^2 \theta) - \frac{2eV_o}{m} \cos \omega t} \quad .$$

Since $v_o^2 \gg eV_o/m$, the angles $\theta$ are not changed to first order by the bunching voltage. (In the formula $V_o$ includes another transit-time factor.) The elapsed time G to Q is

$$t' = \frac{\ell}{v_o\sqrt{1 - \frac{2\,eV_o}{mv_o^2}\cos\omega t}}$$

$$\cong \frac{\ell}{v_o} + B\cos\omega t$$

with $B = (\ell/v_o)(eV_o/mv_o^2)$. This is the ordinary buncher equation. The arrival time at Q is $t' + t + L/v_o$. This is expressed as an arrival phase at Q defined as

$$\phi = \omega t' + \omega t + \frac{\omega\ell}{v_o} + \text{const.}$$

As is well known, it is not possible to make $\phi$ the same for all particles. For our choice of zero phase the "long tails" come from the region $\pi < \omega t < 2\pi$. Note, however, that this region corresponds to negative $\theta$, and hence a beam stop for all (or some) negative $\theta$ eliminates the long tails.

Suppose we make $\phi$ the same for $\omega t = 0, \pi/2, \pi$. Then $B = \pi/2\omega$ and $\phi = \pi/2 + \text{const.}$ for these three particles. Figure 1 shows the arrival phases of all particles from $0 < \omega t < 7\pi/2$. The abscissa is $\omega t$ and the ordinate $\phi = \omega t' + \omega t - \omega\ell/v_o - \pi/2$. If we stop all $\theta < 0$ particles, then all remaining particles (half of the dc beam) arrive at Q within $37^o$ wide phase bands centered at $0, 2\pi, 4\pi, \cdots$. As usual, a compromise between $\ell$, $V_o$, and the energy stability of the dc pre-injector is necessary in order to match the admittance of a given linac.

## 4. Deflector - Redeflector and Two Biased Bunching Gaps

Instead of stopping the beam particles with $\theta < 0$, let us provide separate bunching gaps for the positive $\theta$ and negative $\theta$ beams.

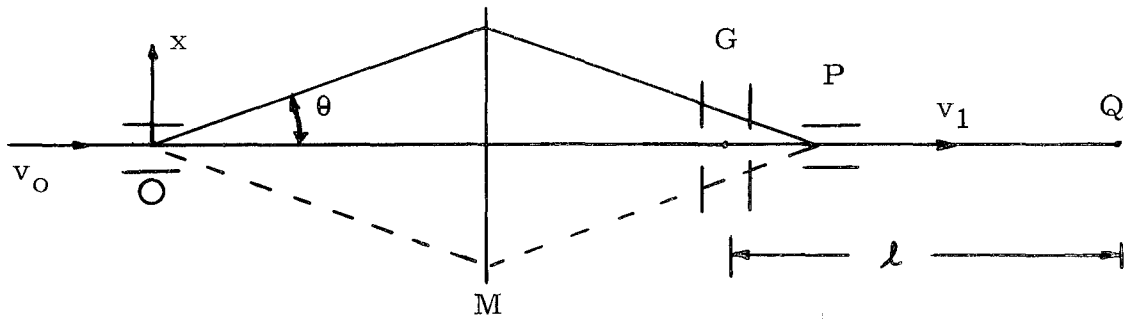


Let gap 1 have voltage $-V_o - V_o \cos \omega t$, for $\theta > 0$
and gap 2 have voltage $V_o + V_o \cos \omega t$, for $\theta < 0$.

The corresponding particle velocities in the drift space GQ are

$$v_1 = \sqrt{v_o^2 - \frac{2eV_o}{m}(1 + \cos \omega t)}, \quad \theta > 0$$

$$v_2 = \sqrt{v_o^2 + \frac{2eV_o}{m}(1 + \cos \omega t)}, \quad \theta < 0$$

and the elapsed times G to Q are

$$t_1' = \frac{\ell}{v_1} = \frac{\ell}{v_o\sqrt{1 - \frac{2eV_o}{mv_o^2}(1 + \cos \omega t)}}$$

$$t_1' \cong \frac{\ell}{v_o} + B(1 + \cos \omega t), \text{ for } \theta > 0, \text{ or } 2n\pi < \omega t < (2n + 1)\pi, \; n = 0, 1, 2 \cdots$$

and

$$t_2' \cong \frac{\ell}{v_o} - B(1 + \cos \omega t), \text{ for } \theta < 0, \text{ or } (2n + 1)\pi < \omega t < (2n + 2)\pi, \; n = 0, 1, 2 \cdots$$

With the choice $B = (\ell/v_o)(eV_o/mv_o^2) = \pi/2\omega$ the arrival phases are the same for $\omega t = 0, \; \pi/2, \; \pi, \; 3\pi/2, \; 2\pi$. Figure 2 shows the arrival phases for all particles as a function of the input phase to the buncher.

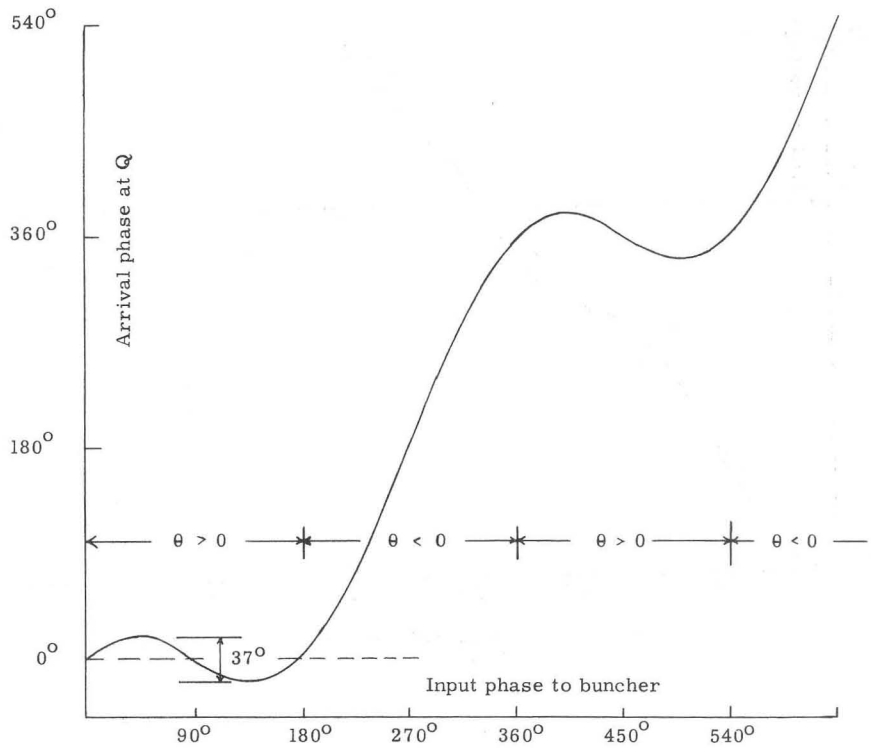


Fig. 1 - Phase of beam particles arriving at Q vs input phase to buncher for a single deflector and bunching gap.

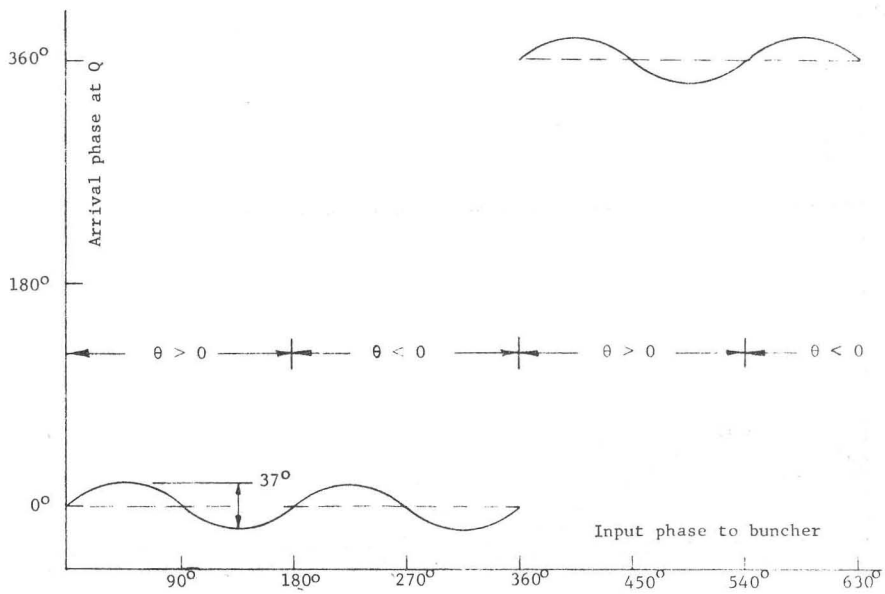


Fig. 2 - Phase of beam particles arriving at Q vs input phase for a two-gap fundamental frequency biased buncher.

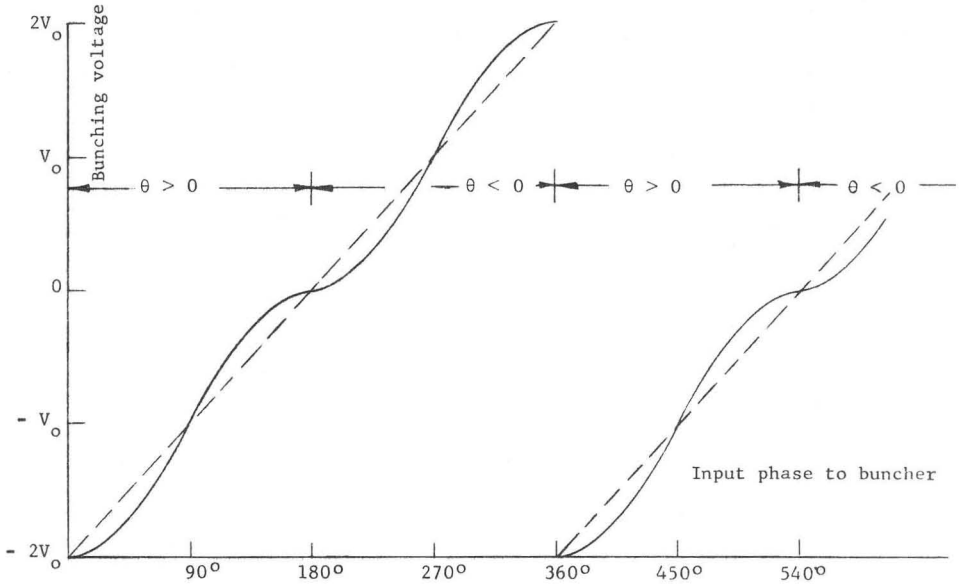


Fig. 3 - Bunching voltage waveshape for a two-gap fundamental frequency biased buncher.

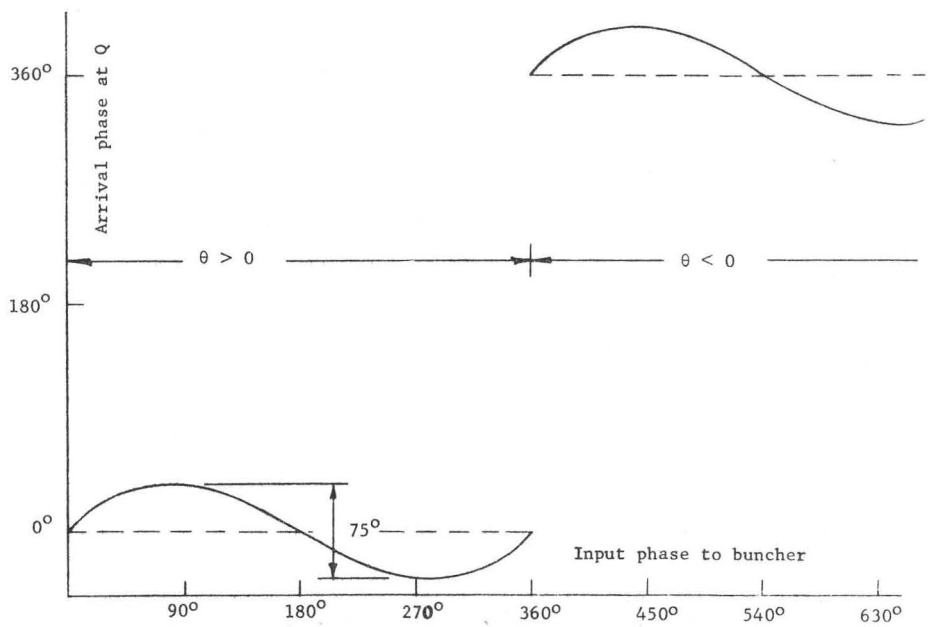


Fig. 4 - Phase of beam particles arriving at Q vs input phase for a two-gap second-subharmonic line-scan buncher.

The abscissa is $\omega t$ and the ordinate $\omega t' + \omega t - \frac{\ell \omega}{v_o} - \pi$. We see that all of the dc beam is bunched into $37^o$ wide phase regions centered at 0, $2\pi$, $4\pi$, $\cdots$. The choice of $V_o$ and $\ell$ is the same as for a conventional buncher.

The reason for the success of this buncher is easily seen if we plot the gap voltage vs input phase. This is shown in Fig. 3, and we see that we have provided nothing more than a good way of approximating a saw-tooth, but not, we note, by conventional Fourier analysis.

The buncher has one nontrivial complication. It requires a dc bias, either $\pm V_o$ for the two legs (or zero and $2 V_o$). These biases cannot be provided with electrostatic fields since the input beam is surrounded by an equipotential surface* (grounded beam pipe) and no arrangement of dc electrodes can accelerate or decelerate such a beam. However, an induction transformer can, in principle, provide a rectangular pulse of accelerating voltage. Since the linac is pulsed, this accelerating pulse should be of comparable duration (say 200 $\mu$sec). In a preliminary look, such a device appears feasible[5] for pulses of the order of 10 kV.

## 5. Subharmonic Deflector and Buncher

The need for dc bias can be eliminated if the alternate halves of input phase corresponding to $\pm \theta$ are bunched into separate linac buckets. This can be done with a subharmonic, $\omega/2$, deflector and buncher.

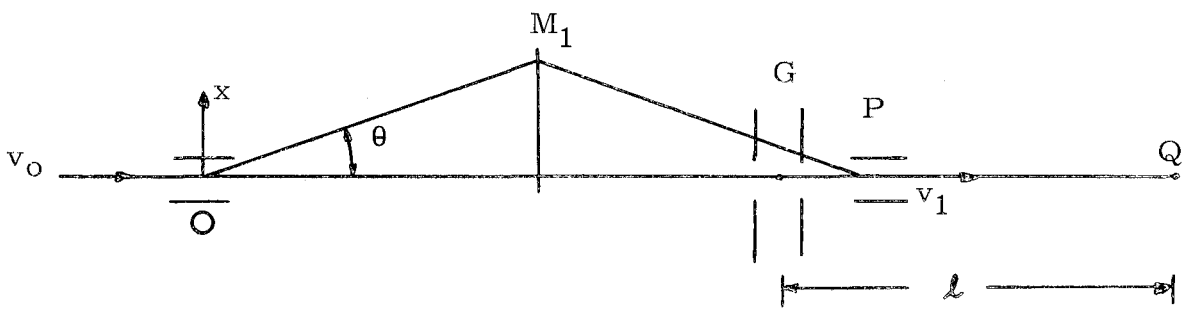


*This condition is imposed by the ion-source and accelerating column of the preinjector. However, one can conceive of devices in which the required dc bias can be provided in the incident beam. A klystron gun is such a device, and klystrons using these bunchers should have greatly improved efficiency.

Let gap 1 have voltage

$$-V_o \cos \frac{\omega}{2} t, \quad \theta > 0 \text{ or } 2n\pi < \frac{\omega}{2} t < (2n+1)\pi, \quad n = 0, 1, 2, \cdots$$

and gap 2 have voltage

$$V_o \cos \frac{\omega}{2} t, \quad \theta < 0 \text{ or } (2n+1)\pi < \frac{\omega}{2} t < (2n+2)\pi, \quad n = 0, 1, 2, \cdots.$$

At P we put a subharmonic redeflector. The elapsed times G to Q are

$$t_1' \cong \frac{\ell}{v_o} + B \cos \frac{\omega}{2} t, \quad \theta > 0$$

$$t_2' \cong \frac{\ell}{v_o} - B \cos \frac{\omega}{2} t, \quad \theta < 0$$

where $B = (\ell/v_o)(eV_o/mv_o^2)$. With the choice $B = \pi/\omega$ the arrival phases are the same for $\omega t = 0, \pi, 2\pi$. Figure 4 shows the arrival phases of all particles as a function of input phase to the buncher. The abscissa is $\omega t$ and the ordinate is $\phi = \omega t' + \omega t - \omega \ell / v_o - \pi$. Figure 5 shows the approximation to the saw-tooth for this case. Note that twice as large a bunching parameter B is required for this arrangement and that twice as large a phase spread ($75^o$) is produced as compared with the biased two-gap buncher.

## 6. Conical-Scan Deflector and Buncher

The essential feature of all of these bunchers is the separation of phase regions in space and the application of appropriately phased sinusoidal bunching voltages to the separated beams. This can be accomplished in a more general way by a two rather than a one-dimensional deflection. In particular, conical-scan deflectors appear promising.

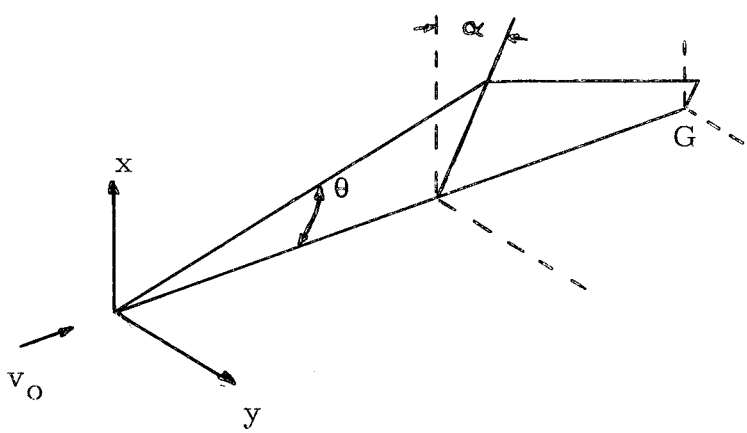

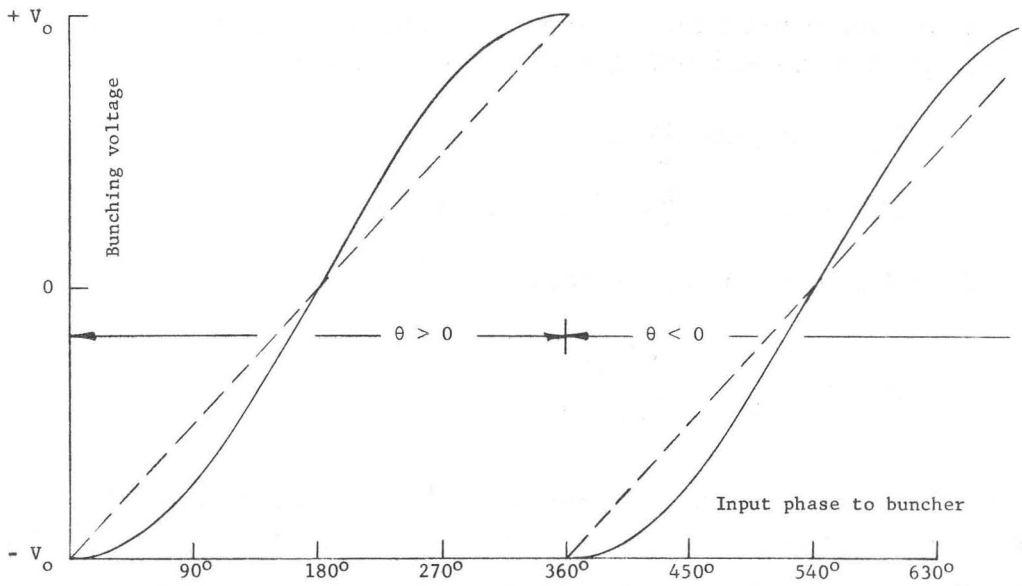


Fig. 5 - Bunching voltage waveshape for two-gap second-subharmonic line-scan buncher.

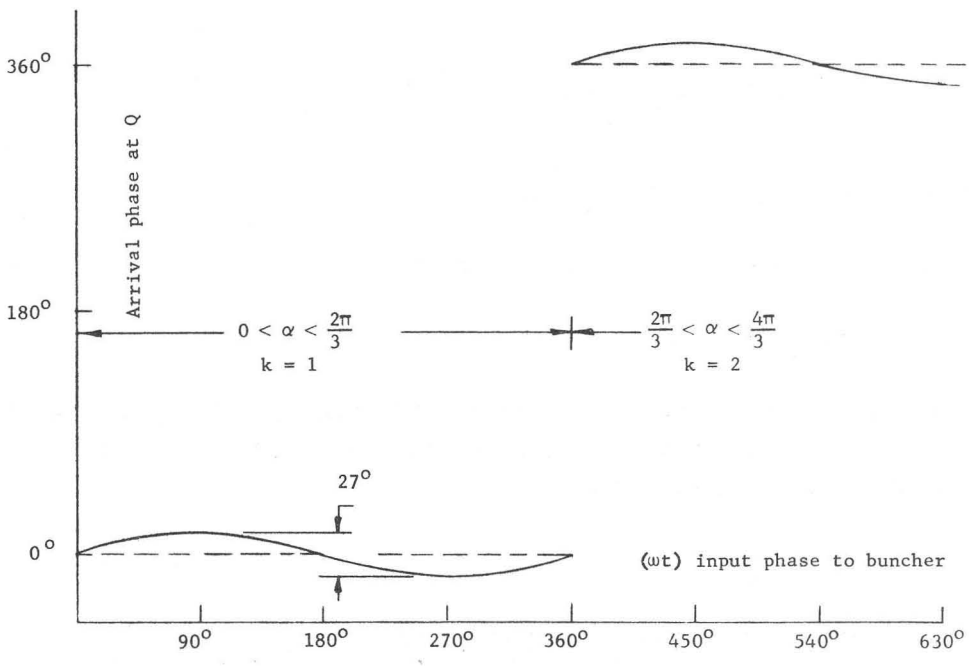


Fig. 6 - Arrival phase for a three-gap third-subharmonic conical-scan buncher.

Consider a deflector at 0 consisting of two perpendicular electric fields in quadrature extending a distance b along z.

$$E_x = E_o \cos \frac{\omega}{p} t$$

$$E_y = E_o \sin \frac{\omega}{p} t , \quad p = 2, 3, \cdots .$$

The deflection angle $\theta$ is constant,

$$\tan \theta = \frac{v_r}{v_o} = \frac{eE_o b}{mv_o^2} ,$$

where b includes a transit-time factor. The azimuth angle of the beam is $\alpha = \frac{\omega t}{p}$, where t is measured when the particle is at 0. The beam is scanned on a cone at uniform angular velocity. A plane parallel to xy at G is divided into p sectors in $\alpha$, each sector containing a bunching gap with voltage

$$gE_z = - V_o \cos \left( \frac{\omega t}{p} - \frac{2 \pi k}{p} + \delta \right) .$$

The gaps are numbered with increasing $\alpha$ by k = 1, 2, $\cdots$ p. Note that after p cycles of the linac frequency $\omega$ the scan repeats exactly. The elapsed time G to Q is

$$t' \cong \frac{\ell}{v_o} + \frac{\ell}{v_o} \frac{eV_o}{mv_o^2} \cos \left( \frac{\omega t}{p} - \frac{2 \pi k}{p} + \delta \right) ,$$

and the arrival phase at Q is

$$\phi = \omega t + \omega t' + \text{const.} = \omega t + \omega B \cos \left( \frac{\omega t}{p} - \frac{2 \pi k}{p} + \delta \right) + C ,$$

with $B = (\ell / v_o)(eV_o / mv_o^2)$.

As in the previous case, the phase shift from gap to gap is so arranged that each $2\pi$ region of $\omega t$ is bunched into a separate linac bucket. The appropriate constants are

$$\delta = \frac{\pi}{p} + \frac{\pi}{2}, \quad C = - \pi , \quad \omega B = \pi / \sin ( \pi / p) .$$

With this choice the arrival phase at Q is

$$\phi = \omega t - \pi + \frac{\pi}{\sin \frac{\pi}{p}} \cos \left[ \frac{\omega t}{p} + \frac{(1 - 2k)\pi}{p} + \frac{\pi}{2} \right].$$

A large p yields a very close approximation to the saw-tooth since the sinusoidal voltage in the gap is being used only in the linear region where it changes sign. Figures 6, 7, 8, 9 show the arrival phase and bunching voltage vs $\omega t$ for p = 3 and p = 4. The p = 2 case is the same as for one-dimensional deflection.

## 7. Bunching Voltage and Drift Length

The conventional choice of bunching voltage and drift length should be re-examined for the very narrow bunches proposed here. For large bunching voltage and short drift length the phase shifts produced by dc voltage fluctuations of the preinjector are small but the velocity spread in the bunched beam is large. An optimum design is a compromise between these.

Assume that an optimum design is one which gives the best beam quality in longitudinal phase space at the input of the first linac tank. For a tank with uniform accelerating field and a bunch which occupies only a small part of the stable longitudinal phase region, the locus of a particle as it undergoes phase oscillations is the ellipse[6]

$$\left( \frac{w - w_s}{w_s} \right)^2 - \frac{2 e E_o T}{m_o c^2 \beta_s} (\phi - \phi_s)^2 \sin \phi_s = \text{const.},$$

where $(w - w_s)$ is the energy deviation for the phase deviation $(\phi - \phi_s)$. The other symbols have the usual meanings. An optimum design fills a given ellipse along both axes and thereby achieves the smallest possible ellipse.

Consider a typical first tank for a proton linac.[7] At its input

$$\omega = 2\pi \ 200 \text{ Mc/s}, \quad \lambda = 1.5 \text{ m}, \quad \phi_s = -30^\circ, \quad E_o = 1.7 \text{ MV/m},$$

$$\beta_s = 0.04, \quad T = 0.9 .$$

For the four-gap buncher the maximum phase error is $7.5^\circ$. Suppose we choose an ellipse with semi-axis $\phi - \phi_s = 10.4^\circ = 0.18$ rad whose other semi-axis is $w - w_s = 19.0$ keV. This determines the bunching voltage, $V_o = \sqrt{2}\ 19.0 = 27$ kV, and the drift length from $\omega B = \sqrt{2}\ \pi = \ell \omega e V_o / m v_o^3$, $\ell = 2.36$ m. We now assume a dc

voltage stability for the preinjector which gives a phase error $10.4^{\circ} - 7.5^{\circ} = 2.9^{\circ}$ in the drift length 2.36 m. The relation is $\Delta\phi = (\omega \ell / v_o)(\Delta v_o / v_o) = 2.9^{\circ}$ giving $\Delta v_o / v_o = 0.204 \times 10^{-3}$ or $\Delta(1/2\, m v_o^2)/(1/2\, m v_o^2) = 0.41 \times 10^{-3}$ which is about the limit of stability of existing Cockcroft-Walton machines. As usual, the energy deviation $\Delta(1/2\, m v_o^2) = 0.31$ keV is a negligible addition to $w - w_s = 19$ keV. The design is an optimum filling of an ellipse of semi-axis $10.4^{\circ}$ for the dc stability cited.

## 8. Second-Order Terms in the Bunch Width

Even an ideal saw-tooth buncher does not produce a bunch of zero phase width.[4] For very narrow widths it is necessary to examine this effect.

For the conical-scan buncher the arrival phase at Q, including second-order terms and for the choice of parameters which gives first-order zeros at $\omega t = 0, \pi, 2\pi$ is

$$\phi = \omega t - \pi + \frac{\pi}{\sin \frac{\pi}{p}} \cos\left(\frac{\omega t}{p} - \frac{2\pi k}{p} + \frac{\pi}{p} + \frac{\pi}{2}\right) + \frac{3 v_o}{2 \omega \ell}\left[\frac{\pi}{\sin \frac{\pi}{p}} \cos\left(\frac{\omega t}{p} - \frac{2\pi k}{p} + \frac{\pi}{p} + \frac{\pi}{2}\right)\right]^2 .$$

The maximum errors in $\phi$ due to the first-order term occur near* $\omega t = \frac{\pi}{2}, \frac{3\pi}{2}$ and are

$$\Delta\phi_1 \cong \pm \pi \left( \frac{\sin(\pi/2p)}{\sin(\pi/p)} - \frac{1}{2} \right) .$$

Errors due to the second-order terms occur at $\omega t = 0, 2\pi$ and are

$$\Delta\phi_2 = \frac{3}{2} \frac{v_o}{\omega \ell} \pi^2 = \frac{3\pi\beta\lambda}{4\ell} .$$

For the four-gap case discussed above $\Delta\phi_1 = \pm 7.5^{\circ}$ and $\Delta\phi_2 = 3.4^{\circ}$. The distorted phase bunch for this case is shown in Fig. 10. There is no net increase in the $15^{\circ}$ phase width but there is some distortion.

*The maximum arrival phase errors occur at those $\omega t$ which are the solutions of $\cos(\omega t/p)\cot(\pi/p) + \sin(\omega t/p) = p/\pi$. For large p, $\omega t \cong 0.42\pi$, $1.58\pi$. The errors themselves are almost the same as at $\pi/2$, $3\pi/2$ for all values of p.

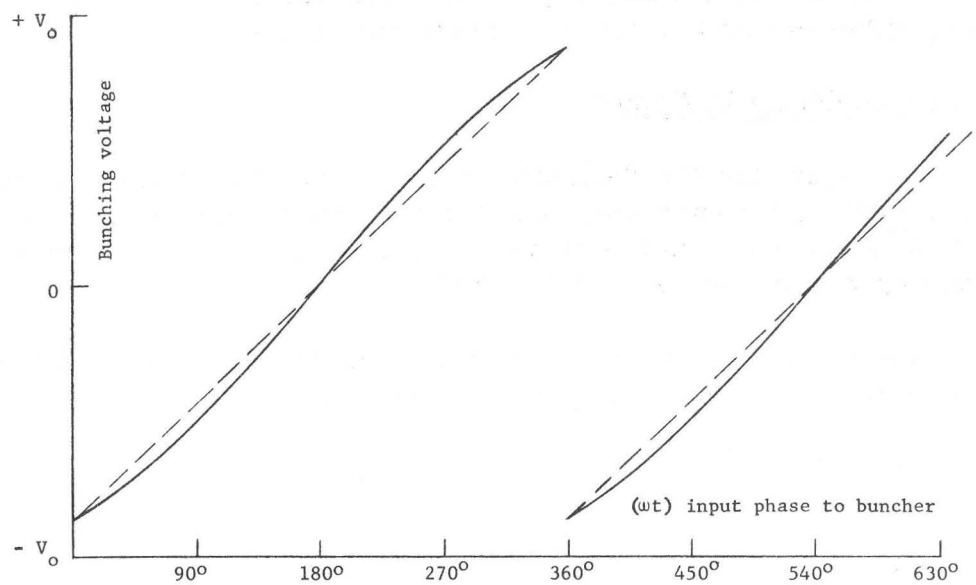


Fig. 7 - Bunching voltage waveshape for a three-gap third-subharmonic conical-scan buncher.

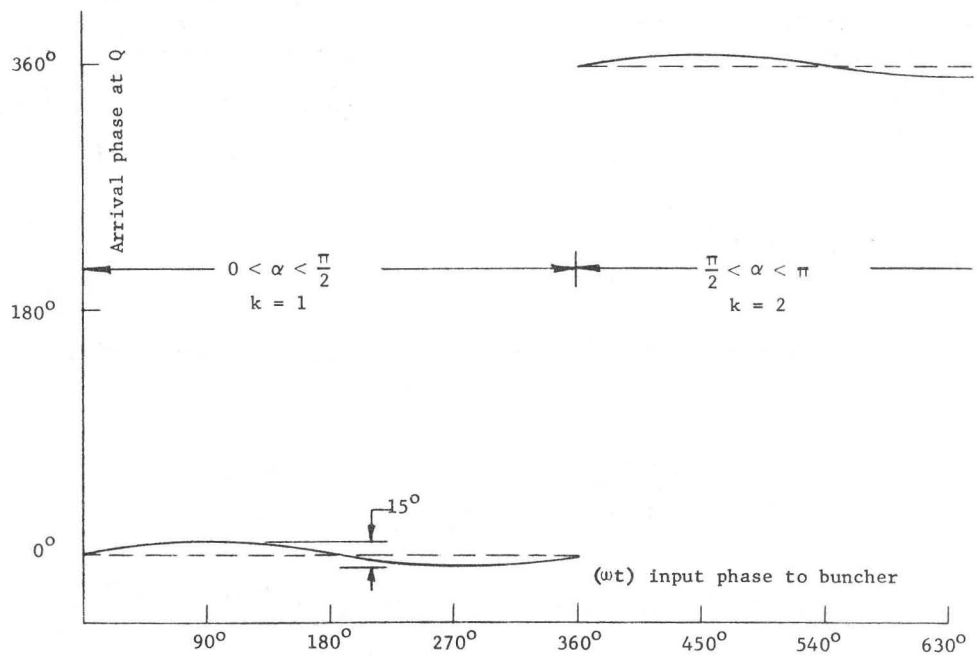


Fig. 8 - Arrival phase for a four-gap fourth-subharmonic conical-scan buncher.

around $\omega t = \pi$ which could be removed by a slightly different choice of the bunching phase and amplitude. In sum, the second-order terms are not negligible but do not seem to cause any trouble.

## 9. Parallel-Plate Deflector

It is clear that the deflection angles should be somewhat larger than the beam emittance angles at the deflector. Since the latter are, say, $0.5^{\circ}$ for a 1 cm radius proton beam at 750 keV, the desired deflection angles are in the range $10^{\circ}$ - $20^{\circ}$.

Consider a one-dimensional deflector consisting of a pair of parallel plates driven by rf voltages balanced to ground.

$$V_2 = -\frac{1}{2} E_o h \cos \frac{\omega t}{p}$$

$$V_4 = \frac{1}{2} E_o h \cos \frac{\omega t}{p} .$$

Ignore, for the present, the longitudinal fields in the end gaps, and consider only the deflection. Measure $t_o$ when the particle reaches 0. The force equation is

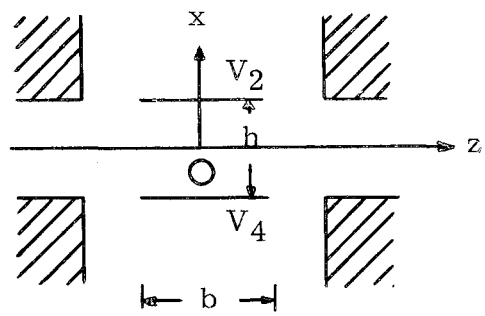


$$m \frac{d^2x}{dt^2} = eE_o \cos \frac{\omega t}{p} .$$

The transverse velocity as the particle leaves the plates at $z = b/2$, $t = t_o + b/2\, v_o$ is

$$v_x = \frac{dx}{dt} = \frac{2\, eE_o p}{m\omega} \sin \frac{\omega b}{2\, p v_o} \cos \frac{\omega t_o}{p} .$$

Maximum deflection for a given $E_o$ occurs for $\frac{\omega b}{p v_o} = \frac{2\pi b}{p \beta_o \lambda} = \pi$ .

For this choice

$$v_x = \frac{dx}{dt} = \frac{2}{\pi} \frac{eE_o b}{m v_o} \cos \frac{\omega t_o}{p}$$

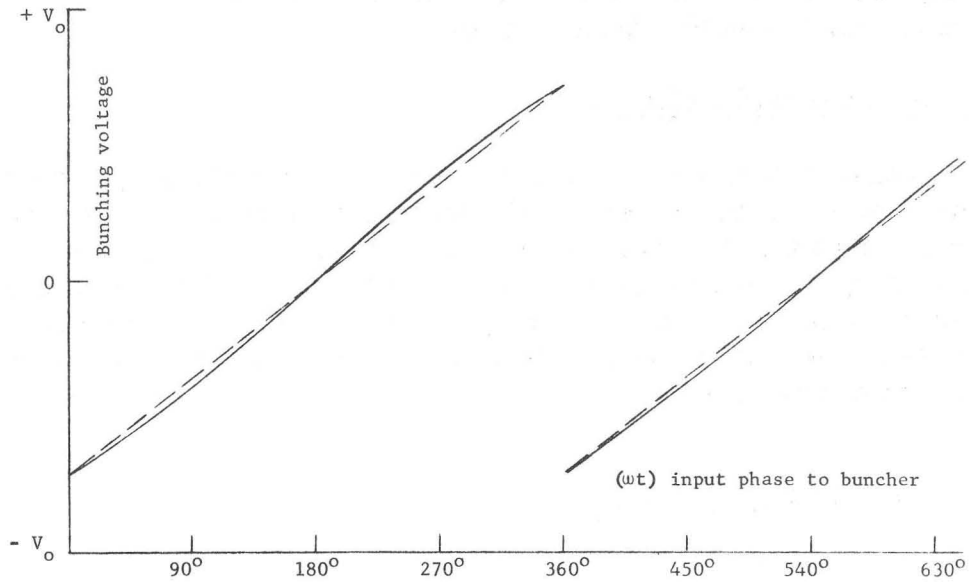


Fig. 9 - Bunching voltage waveshape for a four-gap fourth-subharmonic conical-scan buncher.

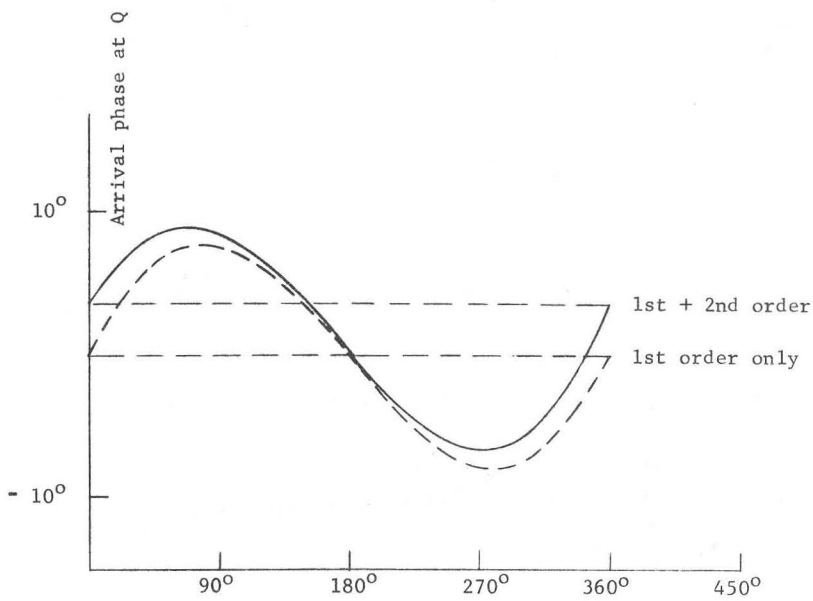


Fig. 10 - Effect of second order terms in a four-gap fourth-subharmonic conical-scan buncher.

For $10^{o}$ maximum deflection with p = 4, $\lambda$ = 1.5 m, $\beta_o$ = 0.04, $E_o$ = 3.4 MV/m and for $20^{o}$, $E_o$ = 7.1 MV/m. These are high but probably attainable field strengths, but they would not be attainable for a fundamental frequency deflector (p = 1).

## 10. Crossed-Field Deflector

A conical scan deflector requires two mutually perpendicular sets of plates (or their equivalent). Consider two such plate sets, with each pair of plates balanced to ground. In general, the mere application of voltages in quadrature will not produce a uniform E field rotating at frequency $\omega/p$, and the uniformity in space and time depends on the electrode shape. A typical case is four equal segments of a circular cylinder with voltages

$$V_1 = -V_3 = -E_o\, a \sin\frac{\omega t}{p}$$

$$V_2 = -V_4 = -E_o\, a \cos\frac{\omega t}{p} .$$

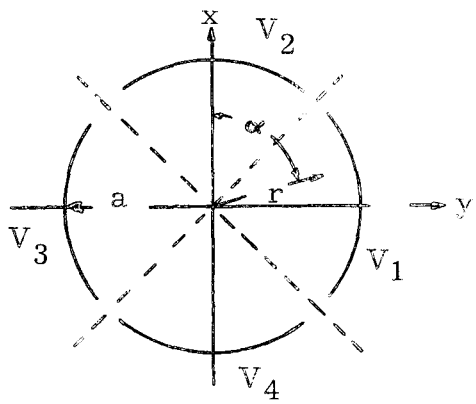


The electrostatic potential at r = a, t = 0 has the boundary value

$$V(\alpha) = \sum_{n=1,3,5\cdots} a_n \cos n\alpha$$

where

$$a_n = \frac{1}{\pi}\int_{-\pi}^{\pi} V(\alpha)\cos n\alpha\, d\alpha = -E_o\, a\,\frac{\sin(n\pi/4)}{(n\pi/4)} .$$

Thus, at r = a and t = t the boundary potential is

$$V(\alpha, t) = -E_o\, a \sum_{n=1,3,5\cdots} \frac{\sin(\frac{n\pi}{4})}{(\frac{n\pi}{4})}\left[\cos n\alpha \cos\frac{\omega t}{p} + \cos n(\alpha - \frac{\pi}{2}) \sin\frac{\omega t}{p}\right] .$$

The potential in the region of the axis can be expanded in terms of dipole, sextupole, etc. terms varying as $(r/a)^1$, $(r/a)^3$, etc. respectively. (Note that even n terms, e.g. quadrupole, are absent.) Thus the deflecting

fields near the axis are

$$E_r = -\frac{\partial V}{\partial r} = E_o \frac{2\sqrt{2}}{\pi}\left[\cos\left(\alpha - \frac{\omega t}{p}\right) + \left(\frac{r}{a}\right)^2 \cos\left(3\alpha + \frac{\omega t}{p}\right)\right.$$

$$\left. - \left(\frac{r}{a}\right)^4 \cos\left(5\alpha - \frac{\omega t}{p}\right) - \left(\frac{r}{a}\right)^6 \cos\left(7\alpha + \frac{\omega t}{p}\right) + \cdots\right],$$

$$E_\alpha = -\frac{1}{r}\frac{\partial V}{\partial \alpha} = E_o \frac{2\sqrt{2}}{\pi}\left[-\sin\left(\alpha - \frac{\omega t}{p}\right) - \left(\frac{r}{a}\right)^2 \sin\left(3\alpha + \frac{\omega t}{p}\right)\right.$$

$$\left. + \left(\frac{r}{a}\right)^4 \sin\left(5\alpha - \frac{\omega t}{p}\right) - \left(\frac{r}{a}\right)^6 \sin\left(7\alpha + \frac{\omega t}{p}\right) + \cdots\right],$$

a series of vectors rotating at increasing rates, with alternate directions of rotation and alternate signs by pairs. The deflection is not truly conical but a scalloped cone depending on the initial radius of the beam particle. Since appreciable gaps in $\alpha$ must be provided to insulate adjacent electrodes, the higher multipoles will be somewhat larger than indicated. On the other hand, since the transit time is an appreciable fraction of a period, the rapid rotation of the higher multipoles will tend to average to zero and, more important, they are small near the axis.

The dynamics of deflection is more conveniently treated in (xy) where the fields are:

$$E_x = E_o \frac{2\sqrt{2}}{\pi}\left\{\cos\frac{\omega t}{p} + \frac{1}{a^2}\left[(x^2 - y^2)\cos\frac{\omega t}{p} - 2xy\sin\frac{\omega t}{p}\right]\right.$$

$$\left. + \frac{1}{a^4}\left[(-x^4 - y^4 + 6x^2y^2)\cos\frac{\omega t}{p} + (4xy^3 - 4x^3y)\sin\frac{\omega t}{p}\right] + \cdots\right\}$$

$$E_y = E_o \frac{2\sqrt{2}}{\pi}\left\{\sin\frac{\omega t}{p} + \frac{1}{a^2}\left[(y^2 - x^2)\frac{\sin\omega t}{p} - 2xy\cos\frac{\omega t}{p}\right]\right.$$

$$\left. + \frac{1}{a^4}\left[(-x^4 - y^4 + 6x^2y^2)\sin\frac{\omega t}{p} + (4x^3y - 4xy^3)\cos\frac{\omega t}{p}\right] + \cdots\right\}$$

The equations of motion

$$m\frac{d^2x}{dt^2} = e E_x$$

$$m\frac{d^2y}{dt^2} = e E_y$$

are coupled and too complicated for exact solution. An approximate solution is obtained by integrating twice for the pure dipole field, substituting these x, y into the sextupole term, and integrating this equation once to obtain the deflection angles. For the transit time $(\omega b/pv_o) = \pi$, the approximate (pure dipole) solutions are

$$m\frac{dx}{dt} = e E_o \frac{2\sqrt{2}}{\pi}\frac{p}{\omega}\left[\sin\frac{\omega t}{p} + \cos\frac{\omega t_o}{p}\right]$$

$$m\frac{dy}{dt} = e E_o \frac{2\sqrt{2}}{\pi}\frac{p}{\omega}\left[-\cos\frac{\omega t}{p} + \sin\frac{\omega t_o}{p}\right]$$

$$m x = e E_o \frac{2\sqrt{2}}{\pi}\frac{p^2}{\omega^2}\left[-\cos\frac{\omega t}{p} + \left(\frac{\omega t}{p} - \frac{\omega t_o}{p} + \frac{\pi}{2}\right)\cos\frac{\omega t_o}{p} + \sin\frac{\omega t_o}{p}\right]$$

$$m y = e E_o \frac{2\sqrt{2}}{\pi}\frac{p^2}{\omega^2}\left[-\sin\frac{\omega t}{p} + \left(\frac{\omega t}{p} - \frac{\omega t_o}{p} + \frac{\pi}{2}\right)\sin\frac{\omega t_o}{p} - \cos\frac{\omega t_o}{p}\right]$$

$$\tan\theta = \frac{e E_o 4\sqrt{2}\, p}{m v_o \pi \omega} = \frac{e E_o b 4\sqrt{2}}{m v_o^2 \pi^2}$$

where $t_o$ is the time at which the particle reaches 0. The effect of the sextupole field is three scallops on the cone of trajectories. The amplitude of the scallops is approximately $\Delta\theta$ where

$$\frac{\Delta\theta}{\tan\theta} = \frac{\pi}{2a^2}\left(\frac{e E_o 2\sqrt{2}\, p^2}{m \pi \omega^2}\right)^2$$

$$= \frac{1}{8\pi}\frac{b^2}{a^2}\tan^2\theta .$$

For $\theta = 10^o$ and a maximum error $\Delta\theta/\tan\theta = 0.1$ the deflector radius must be greater than $b/9$, and if it is $b/3$, the error is 10 times less. The effect is not serious. In any case, a symmetrically placed re-deflector cancels the aberration.

## 11. Parallel Plates in Tandem

There is another solution to the conical scan deflector which uses smaller apertures for a given aberration and hence lower voltages for a given deflection. This consists of two independent sets of parallel plates mutually perpendicular and in tandem. Such a deflector cannot give a cone but it can produce a circular trace at the buncher. The analysis is not given here, being essentially the same as Section 9 above.

## 12. Twisted Parallel-Plate Deflector

Another conical-scan deflector which can be thought of as the limiting case of parallel-plate pairs in tandem is a pair of parallel plates, twisted with a uniform pitch, so that the field rotated uniformly with z. If the plate separation is small as compared with the pitch, the field is approximately uniform

$$E_x = E_o \cos kz \sin\left(\frac{\omega t}{p} + \phi\right)$$

$$E_y = E_o \sin kz \sin\left(\frac{\omega t}{p} + \phi\right).$$

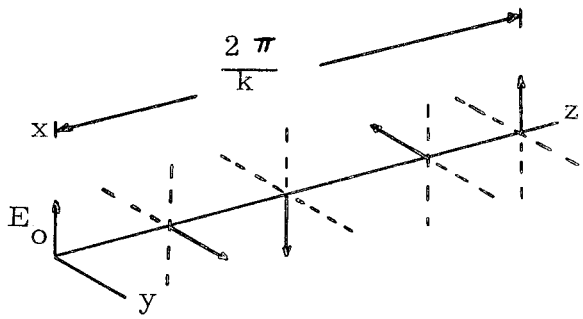


An axial particle of velocity $v_o$ enters the deflector at $t = 0$, $z = 0$ and emerges at $t = T$, $z = b$. The radial velocities at emergence are

$$\dot{x} = \frac{eE_o}{2m}\left\{\left[\frac{1 - \cos\left(\frac{\omega T}{p} + kv_o T\right)}{\frac{\omega}{p} + kv_o} + \frac{1 - \cos\left(\frac{\omega T}{p} - kv_o T\right)}{\frac{\omega}{p} - kv_o}\right]\cos\phi\right.$$

$$\left. + \left[\frac{\sin\left(\frac{\omega T}{p} + kv_o T\right)}{\frac{\omega}{p} + kv_o} + \frac{\sin\left(\frac{\omega T}{p} - kv_o T\right)}{\frac{\omega}{p} - kv_o}\right]\sin\phi\right\}$$

$$\dot{y} = \frac{eE_o}{2m}\left\{\left[\frac{1 - \cos\left(\frac{\omega T}{p} + kv_o T\right)}{\frac{\omega}{p} + kv_o} - \frac{1 - \cos\left(\frac{\omega T}{p} - kv_o T\right)}{\frac{\omega}{p} - kv_o}\right]\sin\phi\right.$$

$$\left. - \left[\frac{\sin\left(\frac{\omega T}{p} + kv_o T\right)}{\frac{\omega}{p} + kv_o} - \frac{\sin\left(\frac{\omega T}{p} - kv_o T\right)}{\frac{\omega}{p} - kv_o}\right]\cos\phi\right\}.$$

For a conical scan $\dot{x}/\dot{y} = \pm \tan(\phi - \phi_o)$ which gives three types of solutions

a) $kv_o = \omega/p$ with $\omega T/p = \pi n$, $n = 1, 2, \cdots$

$$\dot{x} = \frac{eE_o}{2m} \pi n \frac{p}{\omega} \sin \phi$$

$$\dot{y} = \frac{eE_o}{2m} \pi n \frac{p}{\omega} \cos \phi \quad .$$

In this arrangement the velocities continue to grow with the length: the x and y impulses are in step with the particle everywhere, a sort of synchronous deflecting mode.

b) $\omega T/p - kv_o T = 2\pi n$, $n = 1, 2, \cdots$

$$\dot{x} = \frac{eE_o}{2m} \frac{1}{\frac{\omega}{p} + kv_o} \cos (\phi - \phi_o)$$

$$\dot{y} = \frac{eE_o}{2m} \frac{1}{\frac{\omega}{p} + kv_o} \sin (\phi - \phi_o)$$

$$\tan \phi_o = \frac{\sin (\frac{\omega T}{p} + kv_o T)}{1 - \cos (\frac{\omega T}{p} + kv_o T)} \quad .$$

c) $\omega T/p + kv_o T = 2\pi n$, $n = 1, 2, \cdots$

$$\dot{x} = \frac{eE_o}{2m} \frac{1}{\frac{\omega}{p} - kv_o} \cos (\phi - \phi_o)$$

$$\dot{y} = -\frac{eE_o}{2m} \frac{1}{\frac{\omega}{p} - kv_o} \sin (\phi - \phi_o)$$

$$\tan \phi_o = \frac{\sin (\frac{\omega T}{p} - kv_o T)}{1 - \cos (\frac{\omega T}{p} - kv_o T)} \quad .$$

For (b) and (c) the deflection does not grow with n. Solutions (a) give the largest deflections for a given $E_o$ and b, and the deflection of

solutions (c) is the weakest. We also note that the twist is greatest for solutions (a), and the aberrations, which are related to the twist, are largest for (a). However, the synchronous mode (a) seems to be the most attractive for an actual design.

There are two kinds of aberrations produced by a twisted field. One is the lack of conical symmetry of the deflections $(x_1, y_1)$ at emergence even though the velocities are without aberration; this is inherent in the twisted plates in lowest approximation. The second kind is a velocity aberration induced by the nonuniformity of the field across the aperture because of the twist. That is, a twisted uniform field cannot, in fact, be produced because it is not a solution of Laplace's equation. We consider the deflection aberration first.

For solutions (a) with $kv_o = \omega/p$ and $\omega T/p = \pi n$, the deflections at emergence for a uniform, twisted field, are

$$x_1 = \frac{eE_o}{2m} \frac{p^2}{2\omega^2} n\pi (\cos\phi + n\pi \sin\phi)$$

$$y_1 = \frac{eE_o}{2m} \frac{p^2}{2\omega^2} n\pi (\sin\phi + n\pi \cos\phi) .$$

The variation of $r_1 = (x_1^2 + y_1^2)^{1/2}$ with $\phi$ is an aberration. The magnitude of the aberration is

$$\frac{|\Delta r_1|_{max}}{(r_1)_{av.}} = \frac{n\pi}{1 + n^2\pi^2}$$

which is largest for $n = 1$ and varies approximately as $1/n$. Figure 11 shows the deflections for the worst ($n = 1$) case. We note, in particular, that a particle which enters when the field is a maximum ($\phi = \frac{\pi}{2}$) does not undergo a pure x deflection although its radial velocity at emergence is along x. For large n, this distortion disappears and $r_1$ becomes a circle.

While the effect is large in a relative sense for small n, it is not necessarily serious since the deflections $(x_1, y_1)$ are usually small as compared with the deflections produced by drift with velocities $(v_x, v_y)$ which are, in the uniform field approximation, without aberrations.

Now we consider the velocity aberrations. As we mentioned, a twisted uniform field is not a solution of Laplace's equation, but it can be the dominant term in a true solution. Write the potential as

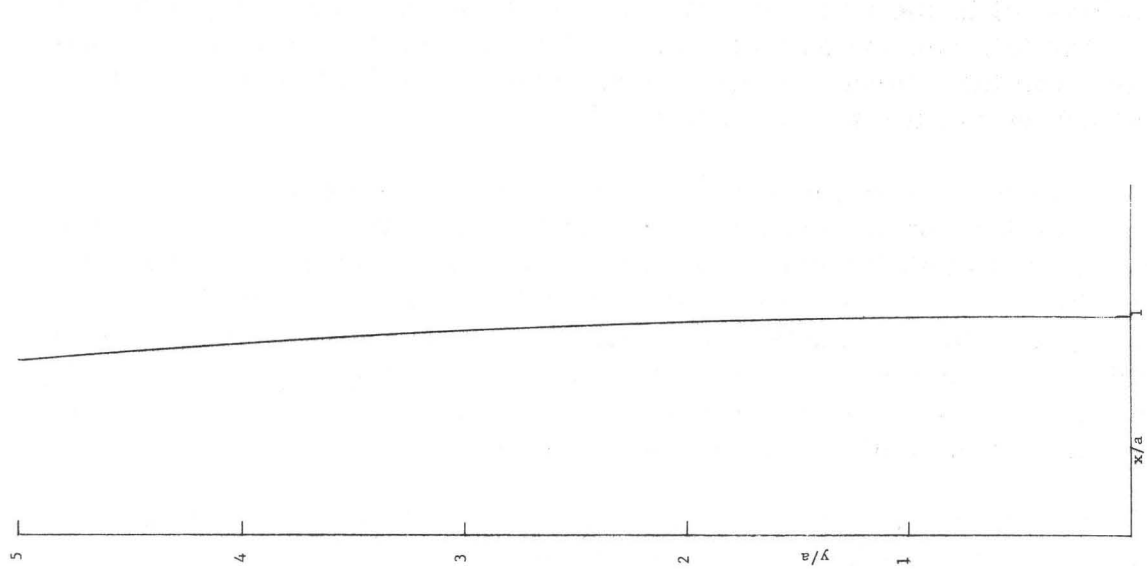


Fig. 12 - Plate shape for a pure $I_1(kr)$ field with $ka = \frac{1}{4}$

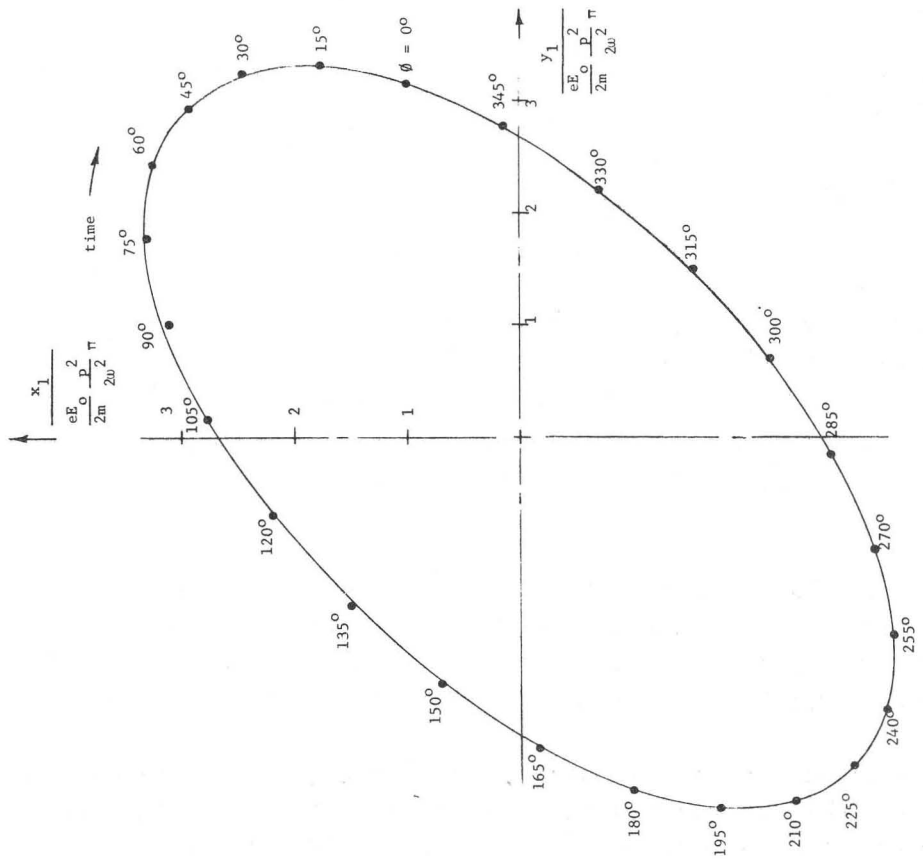


Fig. 11 - Deflections on emergence from twisted plate deflector for n = 1. Points labeled with entrance phase.

$$V = - E_o f(r) \cos (\theta - kz) \sin (\frac{\omega t}{p} + \phi)$$

where $f(r) \rightarrow r$ as $r \rightarrow 0$. With this V, Laplace's equation in cylindrical coordinates is

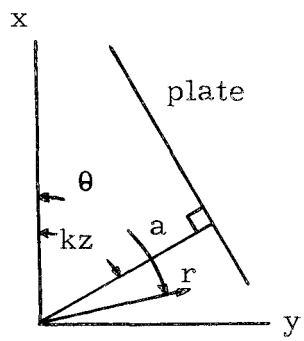


$$\frac{d^2 f}{dr^2} + \frac{1}{r} \frac{df}{dr} - (k^2 + \frac{1}{r^2}) f = 0 ,$$

the modified Bessel equation with solutions

$$f = S_1 I_1 (kr) .$$

Setting the plate potential at $- V_o$ for $\theta = kz$, $r = a$

$$V = - \frac{V_o}{I_1 (ka)} I_1 (kr) \cos (\theta - kz) \sin (\frac{\omega t}{p} + \phi) .$$

If $ka << 0$, $I_1 (ka) \cong ka/2$ and

$$V \cong - V_o \frac{r}{a} \left\{ 1 + \frac{1}{8} k^2 r^2 + \frac{1}{192} k^4 r^4 + \cdots \right\} \cos (\theta - kz) \sin (\frac{\omega t}{p} + \phi) .$$

The plates must be shaped to give this solution, and the polar equation of the plates is obtained by setting $V = - V_o$. Figure 12 shows the plate shape for $2\pi/k = 24$ cm, $a = 3/\pi$ cm, i.e., $ka = 1/4$.

Assume that the plates are shaped to give a pure $I_1 (kr)$ solution. We wish to know the aberration produced by the terms in $r^3$, $r^5$, etc. Keeping only the term in $r^3$

$$E_x = E_o \left\{ \cos kz + \frac{1}{8} k^2 (3 x^2 + y^2) \cos kz \right\} \sin (\frac{\omega t}{p} + \phi)$$

$$E_y = E_o \left\{ \sin kz + \frac{1}{8} k^2 (3 y^2 + x^2) \sin kz \right\} \sin (\frac{\omega t}{p} + \phi) .$$

The equations of motion can be solved, as before, by iteration. When this is done for a twist such that $kv_o = \omega/p$, we find that the emergence velocities are of the form

$$\dot{x} = \frac{eE_o}{m} \frac{p}{\omega} \left\{ \frac{1}{2} n\pi + \frac{1}{8} k^2 \left( \frac{eE_o}{2m} \right)^2 \frac{p^4}{\omega^4} F(\phi) \right\}$$

where $|F(\phi)| < 10$ for all $\phi$. For a $10^o$ deflection with $p = 4$, $n = 1$, the second term is about two thousandths of the first term. The conical aberrations due to the velocity are thus negligible.

Even so, the pure $I_1(kr)$ solution is not the best for small aberrations. Consider the general potential of a uniformly twisted field

$$V = - E_o f(r) \cos n(\theta - kz) \sin \left( \frac{\omega t}{p} + \phi \right)$$

which obeys

$$\frac{d^2 f}{dr^2} + \frac{1}{r} \frac{df}{dr} - \left( n^2 k^2 + \frac{n^2}{r^2} \right) f = 0$$

with solutions

$$f = S_n I_n (n kr), \quad n = 1, 3, 5 \cdots .$$

The general solution is, therefore,

$$V = - \sum_{n=1, 3 \cdots} S_n I_n (n kr) \cos n(\theta - kz) \sin \left( \frac{\omega t}{p} + \phi \right)$$

with

$$\frac{V_o}{E_o} = S_1 I_1 (ka) + S_3 I_3 (3 ka) + \cdots .$$

We can choose the constants $S_n$ in various ways. We can eliminate the terms $r^n \cos(\theta - kz)$ for $n = 3, 5, \cdots$ by setting $S_3 = S_1/27$, $S_5 = S_1/125$, $\cdots$ . The aberrations are then confined to terms of the type $r^n \cos^m(\theta - kz)$ with $n = 3, 5, \cdots$, $m = 3, 5, \cdots n$, with smaller coefficients than with the pure $I_1(kr)$ solution as well as smaller contributions by the integrals. An optimum choice requires detailed computations which we have not carried out.

## 13. Twisted Ribbon Deflector

As we shall see in Section 18, the twisted-plate deflector suffers from an asymmetric fringing field which causes unwanted bunching. This suggests a hybrid device which combines the best features of the twisted-plate and the segmented-cylinder deflectors. It would consist of p conducting ribbons wound helically on a cylinder and driven with the

usual push-pull voltages. The dominant deflecting field would be approximately uniform over the aperture and by rotating in both time and space it could give synchronous deflection.

Write for this dominant term

$$E_x = E_o \cos\left(\frac{\omega t}{p} + kz + \phi\right)$$

$$E_y = E_o \sin\left(\frac{\omega t}{p} + kz + \phi\right) .$$

As written, the expression gives clockwise rotation with t. If $k > 0$, the helix is clockwise also. The synchronous solution occurs for $kv_o = -w/p$. Then, since $z = v_o t$

$$\dot{x} = \frac{eE_o t}{m} \cos\phi$$

$$\dot{y} = \frac{eE_o t}{m} \sin\phi$$

$$x = \frac{eE_o t^2}{2m} \cos\phi$$

$$y = \frac{eE_o t^2}{2m} \sin\phi .$$

The device has unit transit time factor, can be cut to any length, and has E, r, and $\dot{r}$ in phase everywhere. The counter directions of rotation of E in t and z means that the particle sees a uniform E as it proceeds along z. The scan is purely conical.

The device also has other solutions, some of which may be very useful. It is possible to cancel $\dot{r}$ while preserving r and thus to scan conically without radial velocities. This removes the necessity for a lens. An obvious way to do this is to place two identical deflectors in tandem with the second one out of phase by $\pi$ with the first. The second removes the $\dot{r}$ but allows r to grow to twice its value at the exit of the first deflector. At the transition between the two there is a natural bunching gap.

Another way to achieve zero $\dot{r}$ is to operate nonsynchronously. Let $kv_o = -f\omega/p$ where $0 < f < 1$. If we set $(1 - f)\omega T/p = 2\pi n$, where n is an integer and T is the emergence time, we find on emergence that

$$\dot{x}_1 = \dot{y}_1 = 0$$

$$x_1 = -\frac{eE_o}{m}\frac{T^2}{2\pi n}\sin\phi$$

$$y_1 = \frac{eE_o}{m}\frac{T^2}{2\pi n}\cos\phi \ .$$

The deflection is greatest for n = 1. The vector $r_1$ rotates in the same sense as E at emergence and is perpendicular to it, leading by $\pi/2$. If now we place in tandem an identical device, the second out of phase by $\pi$, (i.e. reversed voltages), the particles crossing the gap between them are bunched by the fringing fields between facing electrodes. The bunching is correct (early particles are decelerated) and, with some electrode shaping near the gap, this simple system may incorporate all of the desirable features of a conical scan subharmonic buncher. We have not yet studied any of the more complex features of such a system.

## 14. Rf Drive for Deflectors

The excitation of either the one-dimensional, four-plate conical scan or twisted-plate deflectors should be push-pull, balanced to ground. Since the voltages are high, the circuits should be resonant. In the region of 50 Mc/s where the p = 4 deflector operates, coaxial lines are convenient elements. A possible design can be derived from a half-wave line open at both eneds, with a plate attached to each end and the line folded to bring the plates together. The device is push-pull with respect to the outer conductor. For the four-plate deflector, two such circuits could be arranged to feed two pairs of push-pull plates in time quadrature. Because of the crossed polarization, the interaction will be small even though the E fields occupy the same space.

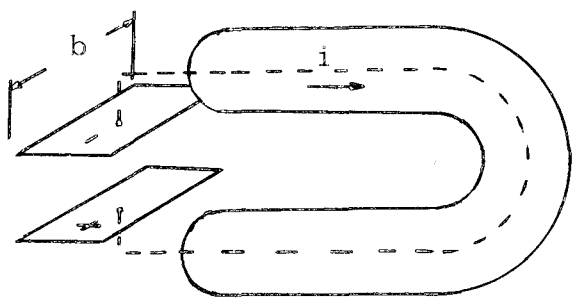

## 15. Lenses

For one-dimensional deflection the lens should be a true lens in the sense that it have the same focal length for all deflection angles. There are a variety of well-known electric and magnetic lenses which have this property for small angles and some which are quite good up to the maximum angles of interest here. In general, they will not be exactly isochonous if they focus exactly, and conversely. These aberrations should be examined in any serious design, but we have not done so.

We have considered in more detail lenses for the conical scan arrangement. Here, since the cone angle is almost constant, the lens may have large aberrations for angles other than the cone angle; the important property to preserve is isochronism as a function of the azimuth angle. Since lenses which are figures of revolution are automatically isochronous in this sense, we have considered two such types which show some promise: coaxial electrostatic systems and magnetic solenoids.

Consider a lens of two coaxial circular cylinders with potentials $\pm V$ of the correct magnitude to give a symmetrical path. The first integral of the equation of motion is

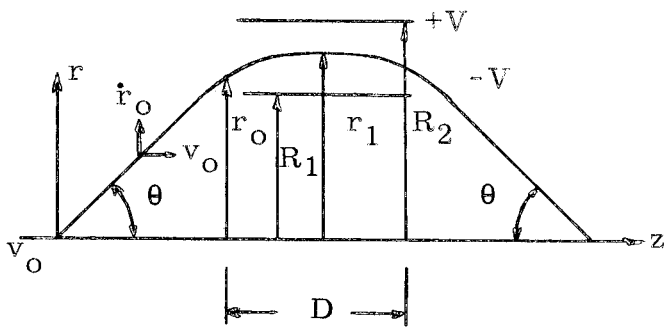


$$\dot{r}^2 - \dot{r}_o^2 = -\frac{4\,eV}{m\,\ell n\,\frac{R_2}{R_1}}\,\ell n\,\frac{r}{r_o},$$

which determines the potential from

$$\frac{2\,eV}{\frac{1}{2}mv_o^2} = \tan^2\theta\,\frac{\ell n\,\frac{R_2}{R_1}}{\ell n\,\frac{r_1}{r_o}}\quad .$$

The second integral can be written

$$\frac{D}{v_o}\sqrt{\frac{eV}{\ell n\,\frac{R_2}{R_1}}} = 2\,r_1\int_o^{w_o} e^{-w^2}\,dw = r_1\sqrt{\pi}\;\mathrm{Erf}\,(w_o)$$

which determines the length D, where $w^2 = \ell n \frac{r_1}{r}$ .

There are many other coaxial systems, all with rather similar properties. For the angles θ of interest here, the well-known concentric-sphere-segment lens is not attractive since it is too short and hence requires very large potentials. There is a large family of shapes intermediate between spheres and cylinders which consist of various arcs rotated around z. None of those examined have any important advantages over the cylinder lens.

All of these coaxial electrostatic systems have one serious technical difficulty - the support of the center electrode which lies completely inside the beam sheath. It could conceivably be cantilevered from a ground plane (perhaps part of the buncher) whose annular beam slot was not complete but rather segmented. This appears very unattractive, particularly if the electrode is at a large negative potential, which requires an insulated cable crossing the beam sheath.

Solenoids avoid this difficulty since the coil can be completely external. Consider a uniform axial field B. A particle deflected through angle θ describes a helix on a cylinder of radius R where

$$B = \frac{mv_o \, c \tan \theta}{eR}$$

and

$$L = \frac{2 \pi R}{\tan \theta} .$$

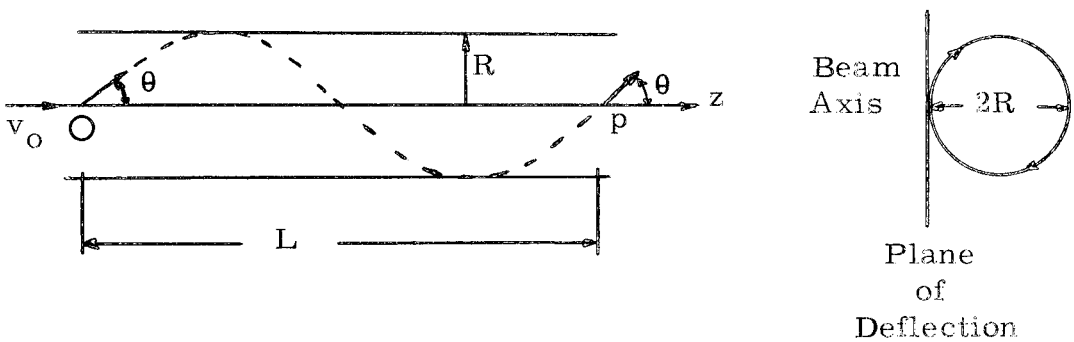

As the beam is scanned conically at frequency $\omega/p$, the cylinder rotates in the same sense and at the same frequency, and the original beam cone is reconstructed at point P. The inside diameter of the solenoid coil must be at least 4 R. The plane of the bunching gaps can be anywhere between P and the 0 to P midpoint, and any radius of the bunching annulus from zero to 2 R can be arranged, depending on this position. For $\theta = 10^{o}$ and $\frac{v_o}{c} = 0.04$ a possible design choice is R = 10 cm, B = 2200 gauss, L = 360 cm. For an air solenoid the required current density in the winding would be about 2400 $A/cm^2$, which is feasible. Iron cladding could improve the efficiency, and there is no necessity for uniformity of B with either r or z so long as the field is axially symmetric.

As a lens, an ideal solenoid reconstructes the input transverse phase space. Thus it acts like a thin lens of unit magnification and focal length L/4.

Lenses which are not figures of revolution, such as electric or magnetic strong focusing triplets, may be sufficiently isochronous. They have one important property; for feasible fields they can have short focal lengths and so permit close spacing between the buncher and redeflector while preserving a large beam radius at the buncher. However, it is just this condition (large $\theta$) which enhances the lack of isochronism. In a serious design these conflicting properties should be studied but we have not done so. As we shall see in the next section, the buncher - redeflector spacing is one of the most difficult problems in the whole scheme, and a successful design must minimize this spacing by a careful choice of the lens system and the transverse beam optics.

## 16. Redeflection Errors

One of the serious difficulties in the whole scheme is the angle errors introduced at the redeflector arising from the fact that the beam is partially bunched when it is redeflected. The errors are small for long drift lengths and short buncher - redeflector spacings but there are technical limits on both of these and near these limits the errors are not negligible.

Consider a conical scan beam converging to P from the bunching gap G. If the bunching is made correct at Q, the arrival phase at P is

$$\phi = t + \frac{z_o}{\ell} \frac{\pi}{\sin \frac{\pi}{p}} \cos \left( \frac{\omega t}{p} - \frac{2\pi k}{p} + \frac{\pi}{p} + \frac{\pi}{2} \right) + C \ .$$

At P the transverse velocities are

$$v_x = - v_o \tan\theta \sin\frac{\omega t}{p}$$

$$v_y = - v_o \tan\theta \cos\frac{\omega t}{p} \quad .$$

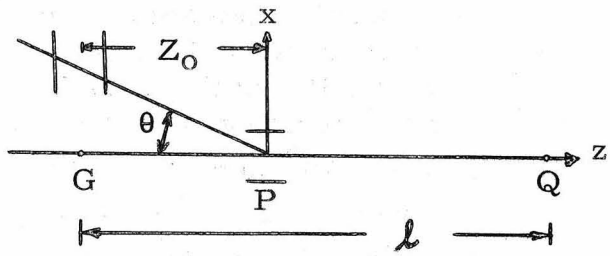


With the redeflector we add the velocities

$$v'_x = v_o \tan\theta' \sin\frac{\phi}{p}$$

$$v'_y = v_o \tan\theta' \cos\frac{\phi}{p} \quad .$$

If $z_o = 0$, $\tan\theta = \tan\theta'$, and $C = 0$, the beam is redeflected without errors. We find that no adjustment of phase (i.e., C) or amplitude (i.e., $\tan\theta'$) reduces the errors, so we remove this generality by setting $C = 0$, $\tan\theta = \tan\theta'$ and write for the angle errors,

$$\Delta\theta_x = \frac{v'_x + v_x}{v_o} = \tan\theta \left(\sin\frac{\phi}{p} - \sin\frac{\omega t}{p}\right)$$

$$\Delta\theta_y = \frac{v'_y + v_y}{v_o} = \tan\theta \left(\cos\frac{\phi}{p} - \cos\frac{\omega t}{p}\right) .$$

Figure 13 shows the angle errors for $p = 4$, $z_o/\ell = 0.1$ as a function of $\frac{\omega t}{p}$ for one complete scan. The points are labeled with $\omega t/p$ values to show the variation in time. The discontinuities in the errors make it essentially impossible to compensate them by changes in the voltage waveform. For the case of Fig. 13 the maximum angle error is $0.078 \tan\theta$ or $0.8^o$ for $\theta = 10^o$.

For angle errors up to a few degrees, the errors are linear in $z_o/\ell$. Thus for $p = 4$, $z_o/\ell = 0.2$ the maximum error is $0.156 \tan\theta$.

These redeflection-angle errors add randomly to the beam emittance angles and hence the transverse phase space of the beam is degraded. This can be serious, depending on the design of the linac and the tolerances on its output beam quality.

Although complex voltage waveforms at the redeflector are not effective in reducing the errors, a second conical scan redeflector near the first linac gap is of some help. At the bunching point Q all of the particles on a single arc of Fig. 13 are essentially simultaneous. The addition of a small deflection voltage equal to the radius of the arc and

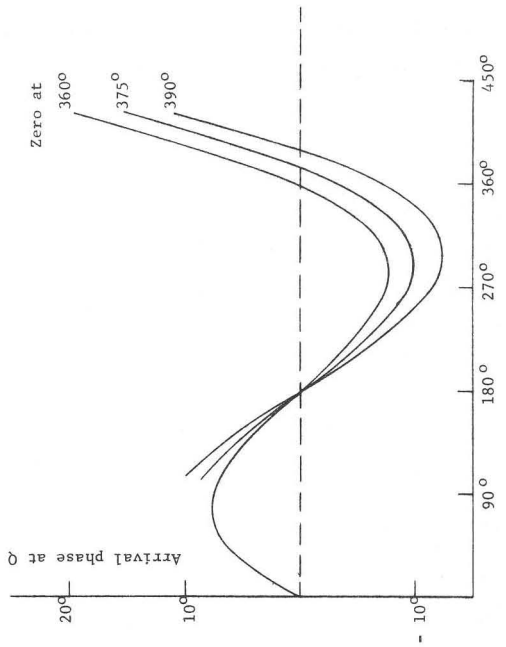


Fig. 14 - Arrival phase for a p = 4 buncher for several choices of the phase at the outer zeros.

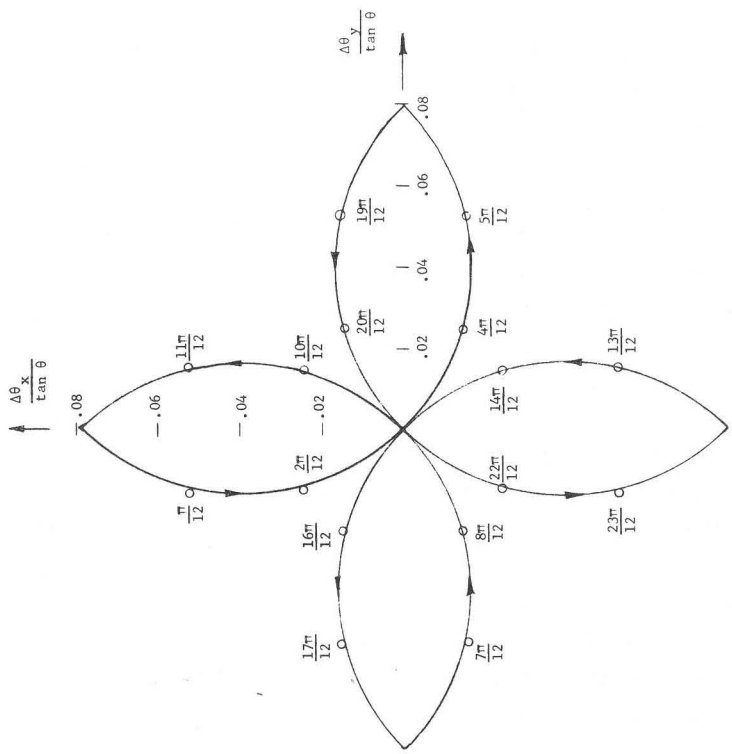


Fig. 13 - Redeflection-angle errors for a fourth-subharmonic conical-scan redeflector located at one-tenth of the drift length for bunching.

of frequency $\omega t/p$ converts Fig. 13 into a circle of radius $0.078 \tan \theta/\sqrt{2}$ and thus reduces the errors by a factor $\sqrt{2}$.

17. The Buncher

For conical deflection the buncher is a set of p annular segments of mean radius $R_B$, each differing in phase from its neighbor by $2\pi/p$, where $\omega/p$ is the scanning and bunching frequency. The ratio of the arc length of a segment to the beam diameter should be large enough so that the beam does not spend too much time overlapping adjacent segments. It is not necessary to reduce this time to an extremely small value since the phase regions just outside the ideal boundaries are no worse than those just inside. For example, for p = 4 (see Fig. 8), the maximum arrival phase error ($7.5^\circ$) which occurs at $\omega t = 285^\circ$ is not exceeded until $\omega t$ reaches $390^\circ$. If it is so arranged that at $\omega t = 360^\circ$ the beam center crosses to the next segment and at $390^\circ$ the trailing edge crosses, then the diameter of the beam is equal to $\frac{\pi}{12} R_B$. If the beam diameter is 1 cm, then $R_B$ must be at least 3.82 cm.

If it is desired to use larger beam diameters (or smaller buncher radii), the arrival phase error can be optimized by choosing a bunching voltage which gives a zero in arrival phase at an $\omega t$ somewhat greater than $360^\circ$ with some sacrifice in the maximum arrival phase error. This is shown in Fig. 14. If, for the p = 4 case, we place the arrival phase zeros at $-15^\circ$, $180^\circ$, $375^\circ$, the maximum arrival phase errors is $\pm 10^\circ$, which is not exceeded until $\omega t$ reaches $408^\circ$. Thus the usable phase overlap is increased from $390^\circ - 360^\circ = 30^\circ$ to $408^\circ - 360^\circ = 48^\circ$ with a corresponding increase in the allowable beam diameter.

For subharmonic bunchers the low frequency and the electrode complexity make drift tube bunchers attractive. For even p the electrodes at opposite ends of a bunching circle diameter are push-pull balanced to ground. Thus the buncher circuits can be the same half-wavelength folded coax that were suggested for the deflector. The two bunching gaps are separated by half a period of $\omega/p$ which is a length $\beta_0 \lambda\, p/2$. For p = 4, the maximum electrode-to-electrode voltage is $\sqrt{2}$ times the voltage to ground and gap $g_2$ must exceed $g_1$. For p = 6, these voltages are equal, and for larger p the electrode-to-electrode voltage continues to diminish. The region of the beam sheath deleted by the gaps $g_2$ can be used on the ground plane for radial straps to support its central disk. Because of the circuit balance, no current flows on these straps. The central annuli of the buncher electrodes require similar straps from the outside annuli; these radial grids will be needed anyhow for good beam dynamics. Such grids will carry current.

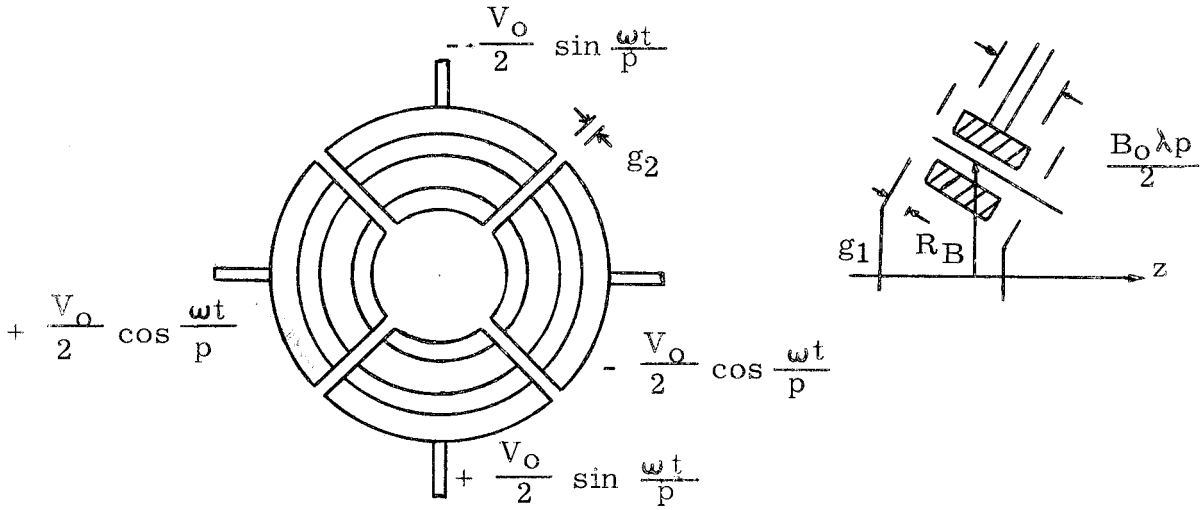


18. Bunching Due to End Effects in the Deflectors

When one attempts to formulate an actual design, it is found that the deflection fields are larger than typical bunching fields. This suggests that the ever present $E_z$ at the ends of a deflector can give a large, and probably undesirable, bunching effect. If we neglect the beam diameter, these effects will occur only at the exit of the deflector and entrance of the redeflector for deflectors which are balanced to ground and hence have $E_z = 0$ on the z axis.

The segmented-cylinder deflector appears to be relatively free of such bunching effects. In the rotating dipole approximation the deflections at emergence (with $\omega b/pv_o = \pi$ ) are

$$x_1 = \frac{eE_o}{m}\frac{2\sqrt{2}}{\pi}\frac{p^2}{\omega^2}\,2\left(\sin\frac{\omega t_o}{p} + \frac{\pi}{2}\cos\frac{\omega t_o}{p}\right)$$

$$y_1 = \frac{eE_o}{m}\frac{2\sqrt{2}}{\pi}\frac{p^2}{\omega^2}\,2\left(-\cos\frac{\omega t_o}{p} + \frac{\pi}{2}\sin\frac{\omega t_o}{p}\right)$$

which is a constant radial deflection rotating around z with frequency $\omega/p$ and a constant phase delay relative to the deflecting field which it

encounters as it emerges. Hence each particle encounters the same fringing field relative to its path and the end effect is equivalent to a dc acceleration and of no importance. The higher multipoles do not behave in this cooperative manner. However, their size can be suppressed by a large aperture-to-deflection ratio and in addition they will fall off more rapidly with z than does the dipole field. We have not actually calculated their residual bunching effects.

The twisted plate deflector has a relatively large and undesirable bunching effect in lowest approximation. The fringing field does not rotate but merely oscillates in time and each ray on the emergent cone receives a different z impulse. Particles which emerge with maximum $\pm$ x deflection traverse the fringing field when it is a time maximum and are decelerated along z, whereas particles with maximum $\pm$ y deflection lie in the plane of zero $E_z$ and also cross near the time zero. The deflector acts like a buncher of frequency $2\omega/p$.

If the z impulses were not too large, they could be compensated in a four-gap buncher by operating the two $\pm$ pairs at different voltages. However, the effect is large. It can be calculated if the fringing field shape is known. For parallel plates spaced by 2 a with potentials $\pm V_o$ the potential is given by a Schwartz-Christoffel transformation of a segmented plane, and can be written

$$\pi \frac{x}{a} = 1 + \ell n \left[ \frac{\pi (V/V_o - z/a)}{\sin \pi (V/V_o + 1)} \right] + \left[ \frac{\pi (V/V_o - z/a)}{\sin \pi (V/V_o + 1)} \right] \cos \pi (V/V_o + 1)$$

where the origin of x, y is in the median plane in-line with the edge of the plates. Figure 15 shows some of the equipotentials and a typical exit trajectory. Since the latter crosses some of the equipotentials, there is a z impulse. For the example shown a numerical integration gives

$$mv_o \Delta v_z \cong - 0.3\ eV_o$$

which is clearly intolerable since $V_o$ is always larger than the peak voltage of the proposed bunchers. It is possible, but unlikely, that plate shaping or auxiliary electrodes in the fringing gap could lower substantially this z impulse. The same conclusions hold for simple one-dimensional deflection by parallel plates.

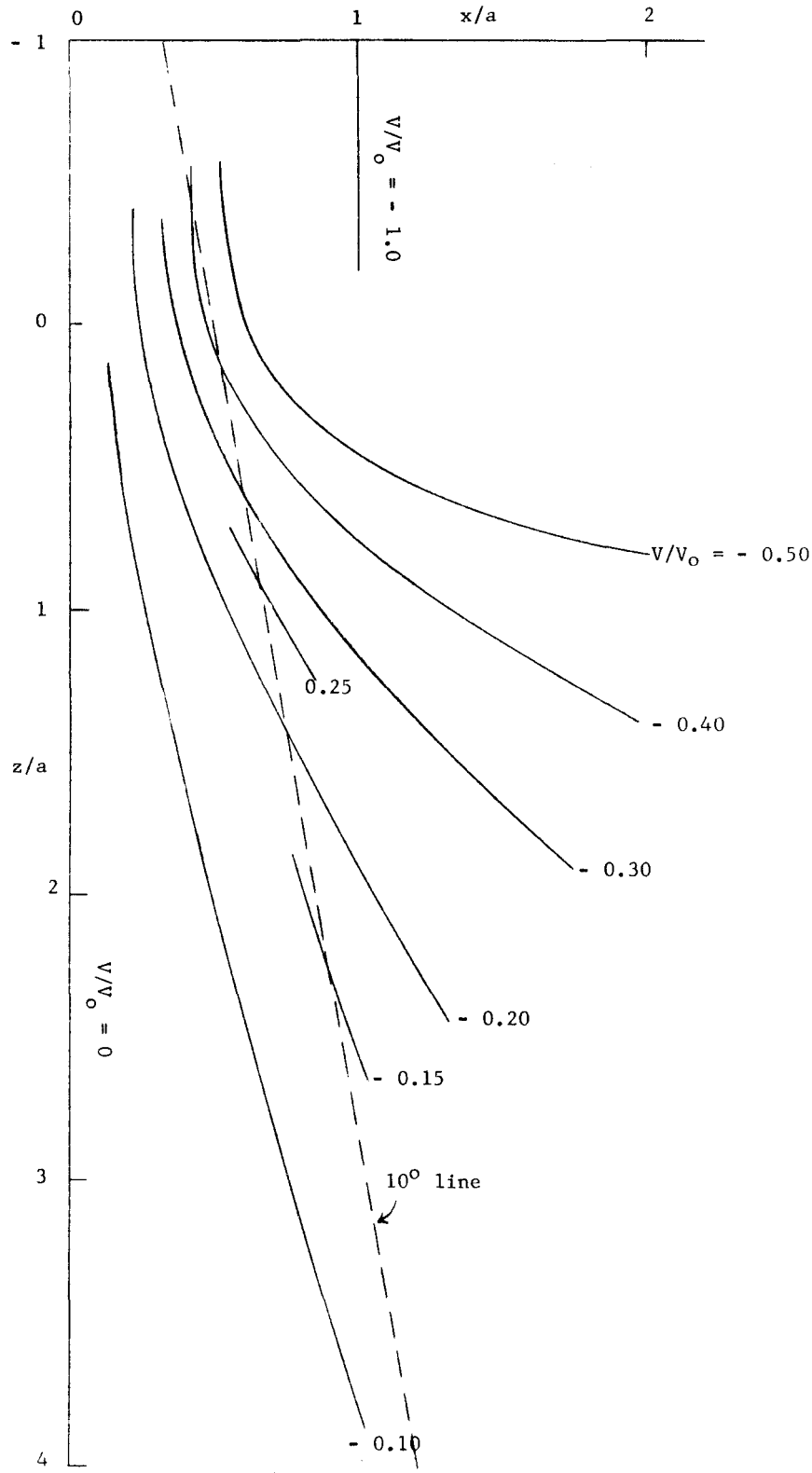
0
1
x/a
2
- 1
0
1
2
3
4
z/a
V/V_o = - 1.0
V/V_o = 0
V/V_o = - 0.50
- 0.40
- 0.30
- 0.25
- 0.20
- 0.15
- 0.10
10° line

Fig. 15

19. Remarks

We have made some attempts to put together the various devices discussed into a system. These attempts have not been very successful because of the conflicting requirements and inadequacies of the components. Chief among these are (a) unwanted bunching by the deflection fields, (b) very high fields in the deflectors, and (c) redeflection errors. It is too early to be sure that these cannot be resolved and it is to be hoped that they can, for the general principle seems both sound and attractive. At this time the simple system of two nonsynchronous twisted ribbon deflectors seems to warrant careful study.

WHEELER: The engineering problems on this tailless buncher are formidable, but a good deal of thought has been given to them and it seems that reasonable solutions are at least possible.

MARTIN, J. H.: I do not want to deviate our discussion too far from linacs, but occasionally linacs are used to feed other machines, such as synchrotrons, and in ours, for example, we would like to be able to chop a beam or do something like this at something like 4 Mc. Now I have also heard of plasma oscillations occurring in ion sources in the few megacycles region and heard of people talking about bona fide chopping devices and so forth. Now I am wondering if anyone has ever tried to take advantage of plasma oscillations in an ion source in such a way that you actually chop the beam at the ion source at frequencies like 5 Mc?

WHEELER: Not that I have heard of.

VAN STEENBERGEN: I think at the AGS we have been most pronouncedly plagued in the past with those particular oscillations and we had a number of observations on them. It is not a single frequency, it is a whole pattern of frequencies and it is not predictable in the sense that one could use a particular frequency.

MARTIN: Well, if this kind of oscillation occurs as in certain kinds of electronic circuitry, you can encourage it to oscillate, usually at one single frequency, so I am proposing here essentially to drive an ion source at a frequency of your choosing and a phase of your choosing.

WHEELER: When are you going to try it ?

MARTIN: Maybe we will get to it.

LAPOSTOLLE: Well, I will only comment to say that this (the tailless buncher) may be a difficult scheme to realize, but it is very similar to an rf separator, and rf separators are being built. I don't think it will be so much of a difficulty to built such a device.

WHEELER: I think its virtues are worth a good deal of effort.

## REFERENCES

1. J. E. Leiss, Conference on Proton Linear Accelerators, Yale University October 21-25, 1963, p. 267.

2. S. Ohnuma, ibid., p. 273.

3. R. Perry, ibid., p. 279.

4. R. Beringer, Yale Design Study Technical Note RB-1, October 26, 1963.

5. M. Plotkin, private communication.

6. L. Smith, Handbuck der Physik, Vol. XLIV, p. 371.

7. Yale Study on High Intensity Proton Accelerators, Final Report, April 1964.